the second profile may be slightly impaired by heat loss from the instrument, although this would not appear in Fig. 1.

Figure 1 shows a region about 50 m thick just below the ice with temperatures in the range −2.13° to −2.16°C; this is close to the freezing point of seawater at these depths. Jacobs *et al.* (*2*) observed salinities of about 34.39 per mil close to the interface. The corresponding freezing point, based on the formula of Fujino *et al.* (*3*), is −2.16°C. Differences between the two profiles are most marked in this region below the interface. There are discontinuities in the profile slopes at about 460 m. Between 400 and 560 m the temperature generally increases with depth, but there are a number of layers from 1 to 10 m thick where the temperature decreases with depth. Below 560 m the temperature is very uniform.

Glaciological evidence indicates that melting occurs at the undersurface of the Ross Ice Shelf near its northern margin. Zumberge (*4*) concluded that the rate of melting decreased toward the south and that freezing might occur in the southern shelf. However, the increase of temperature toward the bottom shown in Fig. 1 suggests that melting is occurring.

Aspects of the hydrology of the Ross Sea have been described by Jacobs *et al.* (*2, 5*). Although a full description of the circulation under the shelf is not available, it is apparent that the water passing under the shelf cannot be much above the freezing point. Because of the high value of the latent heat of melting, for every (net) cubic meter of meltwater produced, there must be many cubic meters of water exchanged across a boundary defined by the northern edge of the Shelf.

Figure 1 is consistent with a circulation in which water flows in from the north at middle depths, heat being transferred through a layer under the ice by convective and mechanical mixing processes, producing meltwater. Because of the net buoyancy production there will be a tendency for the water layer just under the ice to form an outflow.

To stabilize the water column it is required that there be an increase of salinity with depth. The mechanism by which this is produced, and by which heat is transferred upward from the deeper water, is not apparent from the limited data. There seems to be no pronounced "step" structure in the temperature profiles that could be associated with vertical heat transport by processes involving double diffusion.

Below 560 m the profiles indicate very homogeneous water. A straight line was fitted to the data for the lower 20 m of the first profile, using smoothed pressure data. The root-mean-square deviation for the temperature data was about 4×10^{-5} °C and the slope corresponded to a temperature increase with depth of 0.034°C per 10^3 decibars. An approximate value of 0.027°C per 10^3 decibars for the expected adiabatic temperature gradient in well-mixed water was calculated from a formula of Fofonoff (*6*), assuming a salinity of 34.82 per mil based on data from Jacobs *et al.* (*2*).

The presence of this exceptionally well-mixed water would be consistent with the complete breakdown of any stratification in a boundary layer over the seabed. Very homogeneous water is not usually found in the sea except when trapped by a sill, and this is a possibility. Under these conditions geothermal heat flux, which is typically about 4.2×10^{-2} J m^{-2} sec^{-1} ($1 - 10^{-6}$ cal cm^{-2} sec^{-1}), can cause convective mixing.

The fact that there is no water at the seabed as cold as that at the ice-water interface suggests that melting is taking place. It seems reasonable that this should be the case since the sea, with its great capacity for horizontal heat advection, lies below a thick thermally insulating layer of ice. The presence of the well-mixed layer at the seabed is curious unless the flow velocities there are very low.

A. E. GILMOUR
New Zealand Oceanographic Institute, Wellington, New Zealand

References and Notes

1. A. E. Gilmour, *Deep-Sea Res.* **16**, 197 (1969).
2. S. S. Jacobs, A. L. Gordon, J. L. Ardai, Jr., *Science* **203**, 439 (1979).
3. K. Fujino, E. L. Lewis, R. G. Perkins, *J. Geophys. Res.* **79**, 1792 (1974).
4. J. H. Zumberge, *Antarct. Res. Ser.* **2**, 65 (1964).
5. S. S. Jacobs, A. F. Amos, P. M. Bruchhausen, *Deep-Sea Res.* **17**, 935 (1970).
6. N. P. Fofonoff, in *The Sea*, M. N. Hill, Ed. (Wiley, New York, 1962), vol. 1. p. 15.
7. Thanks are expressed to the National Science Foundation, to the RISP staff who made this project possible, and to E. J. Barnes and W. E. Whitley for the electronic design and fieldwork, respectively.

19 May 1978; revised 28 August 1978

Circulation and Melting Beneath the Ross Ice Shelf

Abstract. *Thermohaline observations in the water column beneath the Ross Ice Shelf and along its terminal face show significant vertical stratification, active horizontal circulation, and net melting at the ice shelf base. Heat is supplied by seawater that moves southward beneath the ice shelf from a central warm core and from a western region of high salinity. The near-freezing Ice Shelf Water produced flows northward into the Ross Sea.*

Floating shelves of glacial ice ring half of the Antarctic coastline and constitute nearly 15 percent of the ice sheet. A knowledge of the amount of melting, cooling, and freezing that occurs beneath these ice shelves is important to an understanding of the oceanography of the adjacent oceans, and to the mass balance of the ice sheet (*1*). Oceanographic measurements were made between 15 December 1977 and 3 January 1978 through an access hole melted through the Ross Ice Shelf at 82°22.5′S, 168°37.5′W (J9) (*2*). In the Ross Sea, observations were made along the shelf terminal face (barrier) in December 1976 and January 1978 from the U.S. Coast Guard icebreakers *Northwind* and *Burton Island* (*3*).

The *Northwind* temperature and salinity observations adjacent to the ice shelf (Fig. 1) are similar to other austral summer measurements made from *Burton Island* and *Eltanin* (*4*). The density field is determined primarily by the salinity distribution, and there is less stratification than in temperate and tropical seas. The shallow pycnoclines on stations 31 through 27 and 11 through 10 lie beneath surface water freshened by melted sea (pack) ice. The pycnocline extending from near bottom on station 23 to near surface on station 17 separates water of low salinity on the eastern shelf from water of high salinity (Ross Sea Shelf Water) in the western sector. The latter water mass, which forms primarily from freezing at the sea surface, has the highest salinity and density of any seawater in the Antarctic oceans. It is concentrated in the western Ross Sea by the cyclonic circulation pattern on the continental shelf and by geostrophically induced upwelling along the Victoria Land coast (*5*).

We have observed a warm core of water near the depth of the ice shelf terminal face on three cruises on which measurements were made along the barrier between 170° and 180°W. In Fig. 1 it is approximately 200 km wide and averages 100 m thick, with a mean temperature near 0.5°C above freezing and a salinity near 34.5 per mil. The warm core originates over the continental slope in the upper levels of the Circumpolar Deep Water (*4*). Its position along the barrier

0036-8075/79/0202-0439$00.50/0

appears related to the presence there of density surfaces that have access to both the Circumpolar Deep Water and the ice shelf base. The persistent southerly location of the core and its warm temperature suggest that flow is toward the ice shelf, though such movement need not be continuous. A mean southward flow of 1 cm sec^{-1}, consistent with the calculations below, would carry 10^{11} cal sec^{-1} beneath the ice. For comparison, a vertical geothermal heat flow of 1.3×10^{-6} cal cm^{-2} sec^{-1} (*2*) over the entire 540,000-km^2 (*6*) sea floor beneath the ice shelf would produce 7.0×10^9 cal sec^{-1}. The warm core alone is thus likely to deliver more heat to the sub-ice shelf region than geothermal heat flow, by at least an order of magnitude. A relatively thin region of the ice shelf extends for a few hundred kilometers south of the central barrier (*7*), possibly as a result of increased melting where the warm core first moves beneath the ice.

In two regions along the barrier, subsurface summer temperatures are within 0.2°C of the freezing point in situ. One area extends the full width of the ice shelf, usually at depths near 250 m and salinities between 34.35 and 34.55 per mil. Some of this water may result from sea-surface processes, but it includes stations with temperatures well below the surface freezing point (*Eltanin* 735, for example). The other region is deeper and has salinities near 34.7 per mil. It is

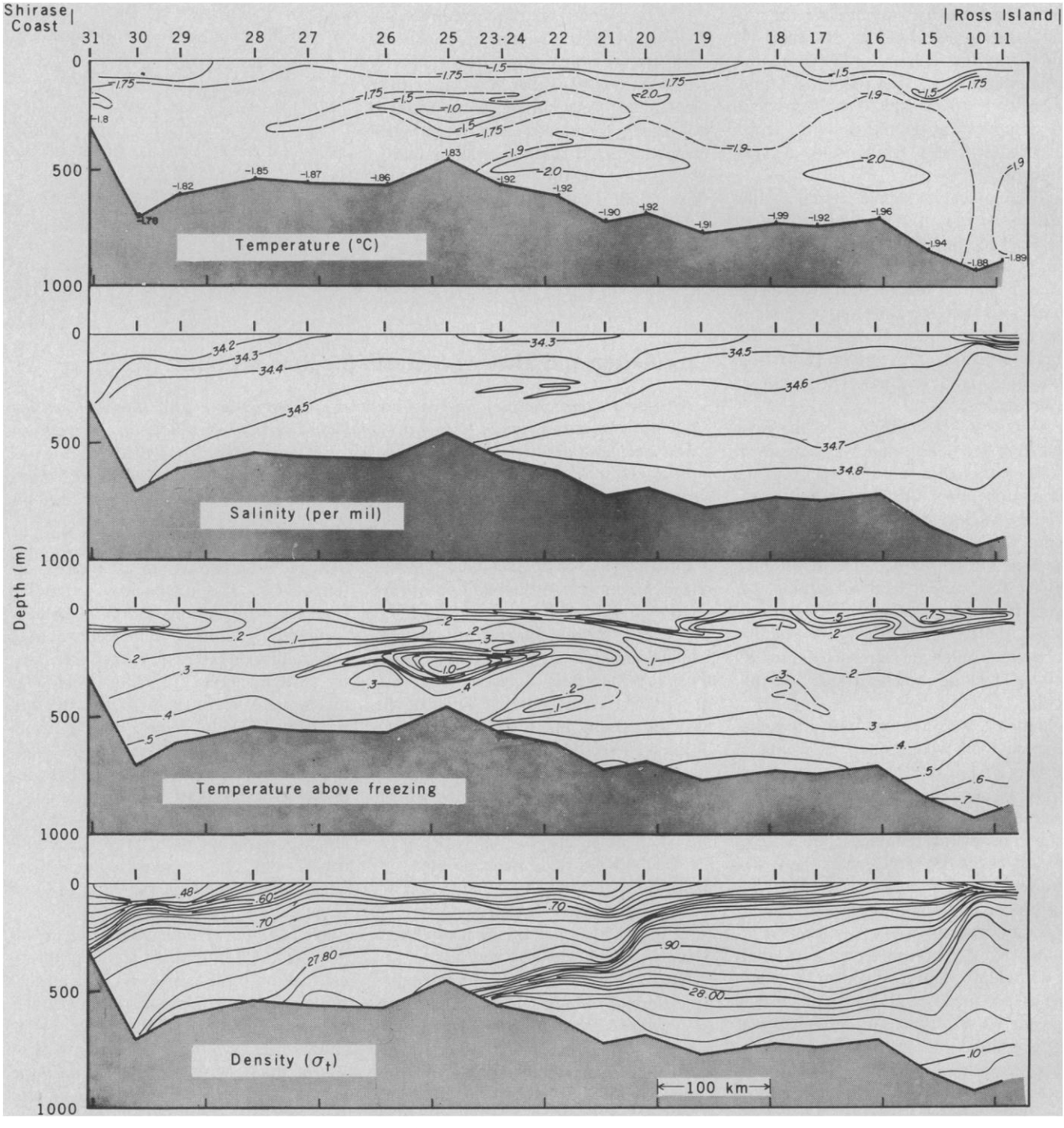

Fig. 1. Temperature, salinity, and density sections from December 1976, *Northwind* stations along the Ross Ice Shelf Barrier (*2*, *3*) (Fig. 2). Temperature above freezing was computed from Fujino *et al.* (*23*). The lower edge of the terminal face of the ice shelf is located at depths of 100 to 250 m (*7*).

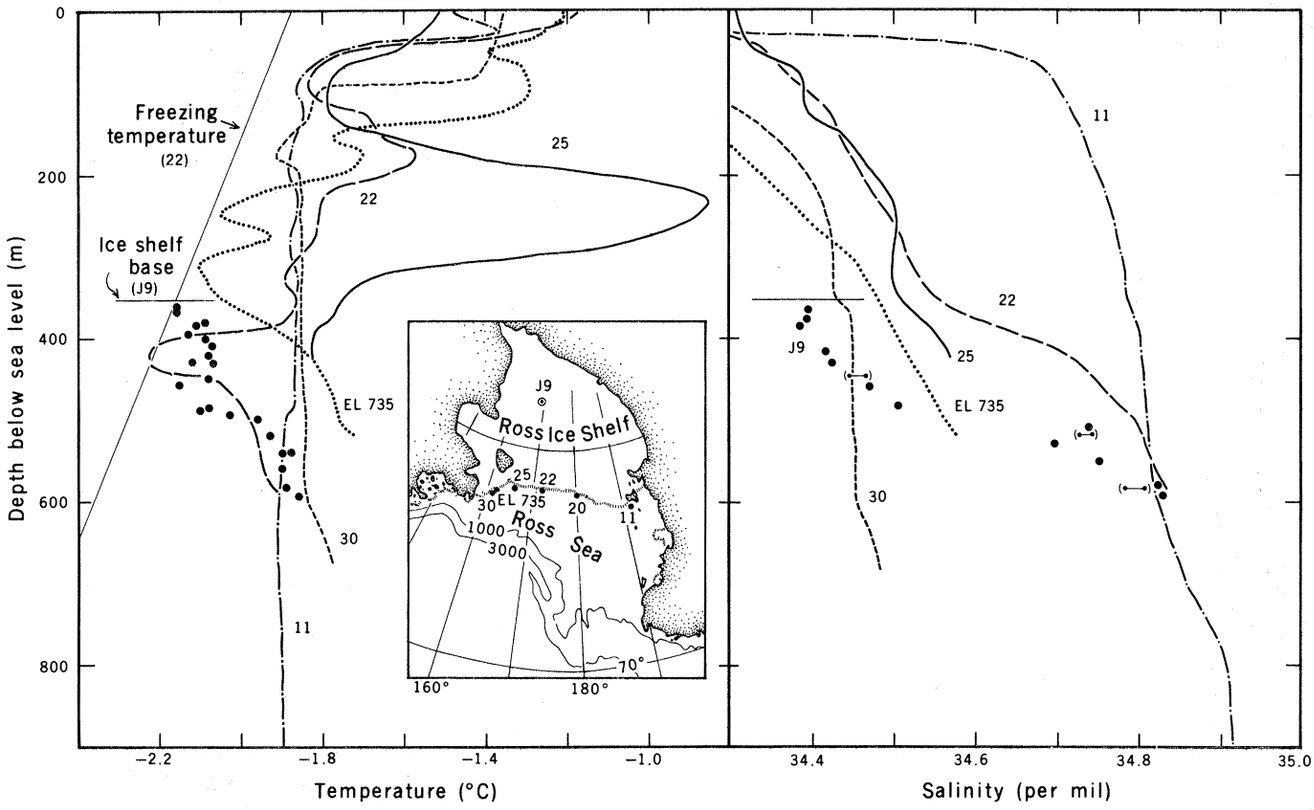

Fig. 2. Temperature and salinity versus depth for representative *Northwind* and *Eltanin* stations along the Ross Ice Shelf Barrier and beneath the shelf at 82°22.5′S, 168°37.5′W (J9). The freezing curve (straight line) is shown for station 22. The freezing curve for other stations will differ very little from that for station 22 because pressure exerts the dominant influence on in situ freezing temperature. The barrier stations (lines with associated station numbers) were taken with salinity-temperature-depth instrumentation. The J9 observations (large dots) represent discrete salinity samples and reversing thermometer observations. The small connected dots are duplicate determinations from the same bottles and illustrate the salinity contamination problem.

centered at station 22 (Fig. 1), but has at other times appeared as far west as *Northwind* 18. The deeper of these Ice Shelf Waters can be traced northward to the continental shelf break (*3*, *4*). A similar water mass exists near the Filchner and Amery ice shelves (*8*).

Beneath the ice shelf at J9, temperature and salinity increased from −2.16°C (the freezing point in situ) and 34.39 per mil at the ice-seawater interface to −1.86°C and 34.83 per mil near the sea floor (Fig. 2). Mixed layers near the bottom and below the ice were separated by an inverse thermocline (*9*), but the stratification was stabilized by a halocline. Temperature varied with time at some depths with a maximum amplitude near 0.05°C at the base of the upper boundary layer (Fig. 2) (*10*). Temperature and salinity characteristics of the bottom boundary layer indicate that it is part of the high-salinity shelf water in the western Ross Sea.

The temporal changes of temperature and salinity within the boundary layer directly below the ice shelf can be determined from the conservation of heat and salt. We assume that meltwater is distributed throughout the upper boundary

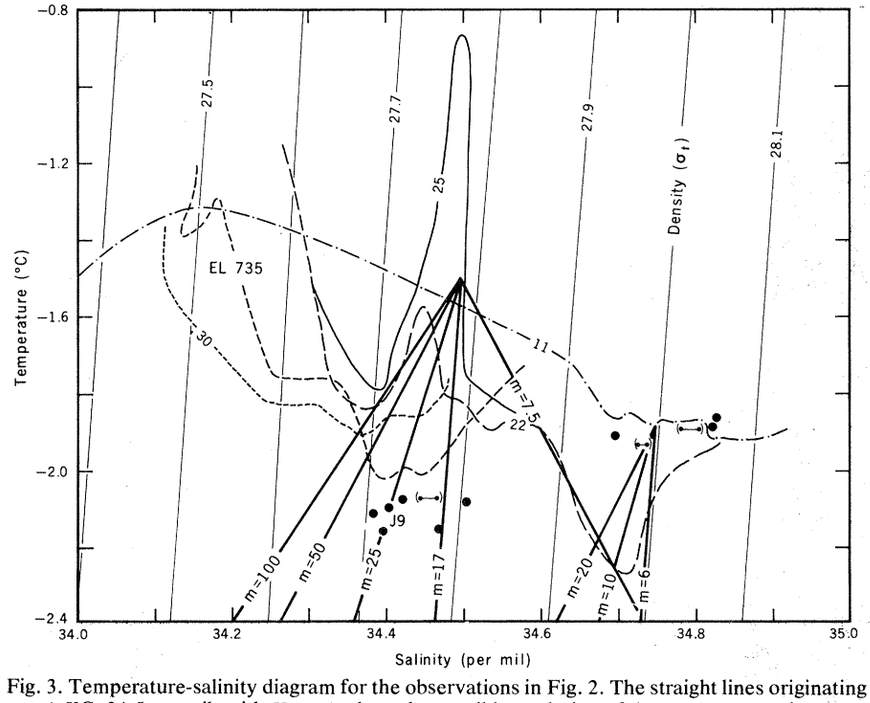

Fig. 3. Temperature-salinity diagram for the observations in Fig. 2. The straight lines originating at −1.5°C, 34.5 per mil, with K_v = 1, show the possible evolution of the warm core as it moves beneath the ice shelf and produces net melting in the amounts shown (in centimeters per year). A melting rate of more than 17 cm per year is necessary to maintain static stability in this boundary layer. The lines originating at −1.9°C, 34.75 per mil, K_v = 1, indicate that the deeper Ice Shelf Water (station 22) can evolve from the western high-salinity shelf water at lower melting rates, with static stability maintained there at 6 cm per year.

layer, which represents that portion of the water column directly interacting with the ice shelf base. Even if melting were as great as 1 m per year, the increase in thickness of this layer would be small compared with its initial vertical extent. At J9, it has about the same thickness as the warm core (station 25). Glaciological data show that ice on the Antarctic continent warms to near the seawater freezing point at bottom (*11*), so further heating over the ocean can be neglected. For flow between the barrier and J9 we can ignore heat flux into the boundary layer from below, since temperature gradients beneath this layer are roughly equal and opposite in sign at each location. Further, we assume that lateral mixing away from the warm core beneath the barrier will simply redistribute water that has been effectively cooled by the ice shelf. The following equations then apply to the vertical thermohaline changes that will occur in the boundary layer beneath the ice:

$$\frac{\Delta T}{\Delta t} = \frac{-\left[\rho_i m L + K_i\left(\frac{\Delta T_i}{\Delta Z}\right)\right]}{C_p \rho_w H} \quad (1)$$

$$\frac{\Delta S}{\Delta t} = \frac{-\left[S\rho_i m - K_v\left(\frac{\Delta S_v}{\Delta Z}\right)\right]}{\rho_w H} \quad (2)$$

where ρ_i is the ice density (0.92 g cm^{-3}); m, melting rate (centimeters in time Δt); L, latent heat of fusion (80 cal g^{-1}); K_i, conductivity of the ice (5.3×10^{-3} cal sec^{-1} cm^{-1} °C^{-1}) (*12*); $\Delta T_i/\Delta Z$, temperature gradient in the lower portion of the ice shelf, averaged between gradients determined from the deepest bore hole and shallowest seawater temperatures at J9 (7.6×10^{-4} °C cm^{-1}) (*2*) and at Little America (27.2×10^{-4} °C cm^{-1}) (*12*); C_p, specific heat of seawater (0.95 cal g^{-1} °C^{-1}); ρ_w, seawater density (1.03 g cm^{-3}); H, boundary layer thickness (7.5×10^3 cm); S, initial salinity (34.5 per mil for the warm core, 34.75 per mil for the upper high-salinity shelf water); K_v, coefficient of vertical turbulent mixing for the halocline beneath the upper boundary layer (1 cal sec^{-1} cm^{-1} °C^{-1}); and $\Delta S_v/\Delta Z$, salinity gradient beneath the boundary layer, averaged from the haloclines at J9 (0.25×10^{-4} per mil cm^{-1}) and below the warm core at station 25 (0.05×10^{-4} per mil cm^{-1}).

Successive terms in the equations indicate that the boundary layer temperature will decrease as oceanic heat is utilized for the phase change from ice to water and for conduction into the ice shelf. The boundary layer salinity will decrease as meltwater is mixed into the layer and increase as a result of turbulent mixing with the halocline below. The ratio of temperature to salinity change,

$$\frac{\Delta T}{\Delta S} = \frac{\left[\rho_i m L + K_i\left(\frac{\Delta T_i}{\Delta Z}\right)\right]}{C_p\left[\rho_i m S - K_v\left(\frac{\Delta S_v}{\Delta Z}\right)\right]} \quad (3)$$

defines a series of lines on a T/S diagram (Fig. 3) along which a water mass can evolve for different linear melting rates. With a K_v of 1, the boundary layer will maintain static stability relative to 400-m density surfaces at a minimum net melting rate of 17 cm per year between the barrier and J9. A line extending from the warm core (34.5 per mil, −1.5°C) through the shallowest J9 observations corresponds to a melting rate of 25 cm per year. The melting rate is sensitive to the choice of K_v, a term that is not well known (*13*). With $K_v = 0.1$, a melting rate of 2 cm per year is sufficient for stability to be maintained.

The melting lines in Fig. 3 do not indicate that a water mass will move along only one line. It is more likely that melting will diminish as the boundary layer moves along an arc of increasing $\Delta T/\Delta S$ beneath the ice shelf (*6*). However, the melting lines do indicate that it is possible by net melting to produce the boundary layer at J9 from the warm core, and the Ice Shelf Water from the upper levels of the high-salinity shelf water. For low melting rates, the boundary layer will become statically unstable and may mix vertically to deeper pressure surfaces. It is possible that the deeper Ice Shelf Water could also form in this manner, for example, with $K_v = 1$ and $m = 7.5$ cm per year.

We can hypothesize the large-scale sub-ice shelf circulation as follows. The warm core flows beneath the ice shelf and undergoes cooling, dilution, and lateral mixing. As the ice shelf thickens, the boundary layer moves to deeper levels and lower freezing temperatures that facilitate melting. Eventually it rises again, with some freezing then possible, and emerges in the Ross Sea as the shallower, low-salinity Ice Shelf Water. Upwelling of this water along the barrier results in supercooling (*14*), as observed on one *Burton Island* station near the ice shelf. High-salinity shelf water flows beneath the western sector of the ice shelf and is cooled and diluted. There the deeper, higher-salinity Ice Shelf Water is produced, with subsequent lateral flow northward to the vicinity of the continental shelf break. Experiments on melting ice in a stratified fluid have also shown lateral spreading of the meltwater and little or no vertical motion (*15*). In particular, early experiments by Pettersson and Sandstrom (*15a*) modeled a thermohaline circulation with some striking resemblances to features we have observed north of the Ross Ice Shelf, including both the warm core and the Ice Shelf Water.

A significant accumulation of frozen seawater has been reported at the base of the Amery and Ross ice shelves (*16*). Freezing is likely in tide cracks that exist at least regionally in the ice shelf base (*17*). Freezing would also occur where a boundary layer at the in situ freezing temperature shoaled beneath a thinning ice sheet (*18*). With the strong pressure dependence of the freezing temperature, vertical movements of the boundary layer may effectively smooth irregularities in the base of the ice shelf by alternate melting and freezing. This process would depend on inflow from the Ross Sea, tidal motions, internal waves, ice shelf bottom roughness and slope, and vertical turbulent mixing. Density lines (Fig. 3) connect the higher-salinity water masses in the western sector at significantly lower melting rates than in the eastern Ross Sea. The probability is therefore greater that more freezing occurs beneath the western side of the ice shelf, as suggested by recent radio-echo sounding data (*18*).

The low heat conductivity of the shelf ice and the observed salinities of the Ice Shelf Water severely restrict the amount of basal freezing that can occur. Upward heat flux into the ice shelf, from the averaged J9 and Little America data, would allow a maximum freezing rate of 3.5 cm per year. The resulting brine would increase the mixed layer salinity by ≈ .016 per mil. By this means it would require 18.8 years for the cold fresh layer at J9 to attain the high salinity of the deeper, 34.7 per mil Ice Shelf Water. Alternatively, net melting of the same magnitude from heat available in the high-salinity shelf water could produce the deeper Ice Shelf Water in only 3.1 years. Biological observations suggest an active circulation beneath the ice shelf (*20*), as do our short-term current measurements with amplitudes as great as 18 cm sec^{-1}. From Eq. 1 we can estimate the time it would take for the upper boundary layer to move from the barrier to J9. With a layer thickness of 75 m (Fig. 2) (*9*), a ΔT of −0.6°C (Fig. 2), and a melting rate of 25 cm sec^{-1} (Fig. 3), then $\Delta t = 2.1$ years. This time interval would in turn require a conservative net southward velocity of only 0.7 cm sec^{-1}. The oceanographic evidence thus indicates that melting at

the ice shelf base is the predominant phase change there, a conclusion that supports some earlier estimates from glaciological data (*1, 21*) and from laboratory and theoretical models (*12, 15a, 22*).

STANLEY S. JACOBS
ARNOLD L. GORDON, J. L. ARDAI, JR.
Lamont-Doherty Geological Observatory of Columbia University, Palisades, New York 10964

References and Notes

1. R. Thomas and P. Coslett, *Nature (London)* **228**, 47 (1970).
2. J. W. Clough and B. L. Hansen, *Science* **203**, 433 (1979). At J9, samples were obtained with modified water sampling bottles (General Oceanics) [E. Suckling, *Exposure* **3** (1975)], and from water pumped from several levels beneath the ice. Problems arising from slush ice and drilling fluid (Diesel Fuel Arctic) in the access hole lowered the quality of some salinity data. Several very low salinities near the ice shelf base are believed to have resulted from contamination from the hole, and are not reported. Temperature and depth observations were taken with low-range, deep-sea reversing thermometers.
3. In the Ross Sea, salinity-temperature-depth instruments (Plessey) were used; the data were corrected to simultaneous measurements obtained with water sampling bottles and thermometers [S. S. Jacobs, *Antarct. J. U.S.* **12**, 43 (1977); _____, P. Bruchhausen, J. Ardai, *ibid.*, in press].
4. S. S. Jacobs, A. F. Amos, P. M. Bruchhausen, *Deep-Sea Res.* **17**, 935 (1970).
5. P. Killworth, *ibid.* **21**, 815 (1974).
6. J. H. Zumberge and C. Swithinbank, *Antarct. Res. Geophys. Monogr. Am. Geophys. Union* 7, 197 (1962).
7. U.S. Geological Survey, *Chart of the Ross Ice Shelf* (Department of the Interior, Washington, D.C., 1972).
8. E. Carmack and T. Foster, *Deep-Sea Res.* **22**, 77 (1975); A. Zverev, *Sov. Antarct. Exped. Inf. Bull.* **1**, 269 (1964).
9. A. E. Gilmour, *Science* **203**, 438 (1979).
10. I. A. Zotikov and V. Zagarodnov, unpublished data.
11. H. Ueda and D. Garfield, in *International Symposium on Antarctic Glaciological Exploration (ISAGE)*, A. J. Gow, C. Keeler, C. C. Langway, W. F. Weeks, Eds. (Hanover, N.H., 1968), pp. 53–68.
12. H. Wexler, *J. Glaciol.* **3**, 626 (1960).
13. C. Garrett, paper presented at the Joint Oceanographic Committee/Scientific Committee on Oceanic Research Conference on General Circulation models of the oceans and their relation to climate, Helsinki, 23 to 27 May 1977.
14. A. Foldvik and T. Kvinge, in *Polar Oceans*, M. Dunbar, Ed. (Arctic Institute of America, Calgary, 1977).
15. H. E. Huppert and J. S. Turner, *Nature (London)* **271**, 46 (1978).
15a. O. Pettersson, *Geogr. J.* **24**, 285 (1904); J. W. Sandstrom, in *Investigations in the Gulf of St. Lawrence and Atlantic Waters off Canada*, J. Hjort, Ed. (Department of Naval Service, Ottawa, 1919), p. 245.
16. V. Morgan, *Nature (London)* **238**, 393 (1972). The fabric, color, salty taste, and inclusions in the lower 6 m of an ice core obtained through the Ross Ice Shelf at J9 suggest a marine origin (I. Zotikov and J. Clough, by telegram to the University of Nebraska, 13 December 1978).
17. J. W. Clough, *Antarct. J. U.S.* **9**, 159 (1974).
18. A. Gordon, in "RISP science plan" (University of Nebraska, Lincoln, 1974), pp. 41–58.
19. C. Neal, paper presented at the Symposium on Dynamics of Large Ice Masses, Ottawa, 21 to 25 August 1978; *J. Glaciol.*, in press.
20. P. M. Bruchhausen, J. A. Raymond, S. S. Jacobs, A. L. DeVries, E. M. Thorndike, H. H. DeWitt, *Science* **203**, 449 (1979).
21. A. P. Crary, E. S. Robinson, H. F. Bennett, W. W. Boyd, Jr., *J. Geophys. Res.* **67**, 2791 (1962); P. A. Shumskiy and I. A. Zotikov, *UGGI, Assoc. Hydrol. Sci. Gen. Assembly Berkeley* (1963), pp. 225–231. Melting has also been calculated for the Erebus Glacier Tongue in McMurdo Sound [G. Holdsworth, *J. Glaciol.* **13**, 27 (1974)].
22. S. Martin and P. Kauffman, *J. Phys. Oceanogr.* **7**, 272 (1977).
23. K. Fujino, E. L. Lewis, R. G. Perkins, *J. Geophys. Res.* **79**, 1792 (1974).
24. We thank the personnel of U.S. Coast Guard icebreakers *Northwind* and *Burton Island*; Ross Ice Shelf Project drillers from Browning Engineering, the University of Nebraska, and the U.S. Army Cold Regions Research and Engineering Laboratory; and P. Bruchhausen, A. Amos, P. McDonald, and M. Rodman for field assistance. Several colleagues, in particular E. Molinelli, made helpful comments on the manuscript. This work was supported by NSF Office of Polar Programs grants C-726 to the University of Nebraska and 76-11872 and 77-22209 to Columbia University. Lamont-Doherty Geological Observatory contribution No. 2776.

12 July 1978; revised 26 September 1978

Ocean Tide and Waves Beneath the Ross Ice Shelf, Antarctica

Abstract. *The ocean tide in the southern Ross Sea is principally diurnal. The tropic tide range (double amplitude) is between 1 and 2 meters, depending on the location, and is closely related to the local water-layer thickness. The range of the tropic tide is more than three times the range of the equatorial tide. Cotidal and coamplitude charts were made for the largest diurnal constituents,* K_1 *and* O_1*, and a provisional cotidal map was made for the semidiurnal constituent* M_2*. The amplitudes of the diurnal tide constituents are larger in the Ross Sea than in the adjacent southern Pacific Ocean, indicating the existence of a diurnal resonance related to the shape and depth of the sea. Waves related to ocean swell propagate into the ice-covered region from the northern Ross Sea. These waves have amplitudes near 1 centimeter, and periods in the range 1 to 15 minutes. The speed at which these waves travel is successfully predicted by flexural wave theory.*

Tidal water movement beneath the Ross Ice Shelf causes diurnal changes in the elevation of the ice surface of as much as 2 m. Beginning in 1973, we undertook a study of the ocean tide in this region as part of the Ross Ice Shelf Project (RISP).

The Ross Sea is a marine embayment penetrating more than 1000 km into the Pacific sector of the Antarctic continent (Fig. 1). The southern part of this sea is covered by the Ross Ice Shelf, a tabular mass of floating ice that extends over about 560,000 km², and is almost everywhere 300 to 600 m thick. The thick ice cover presents an obstacle to the use of conventional tide gauges. In this study we used gravity meters to make measurements of the height of the ocean tide in an unusual way. Tidal fluctuations of

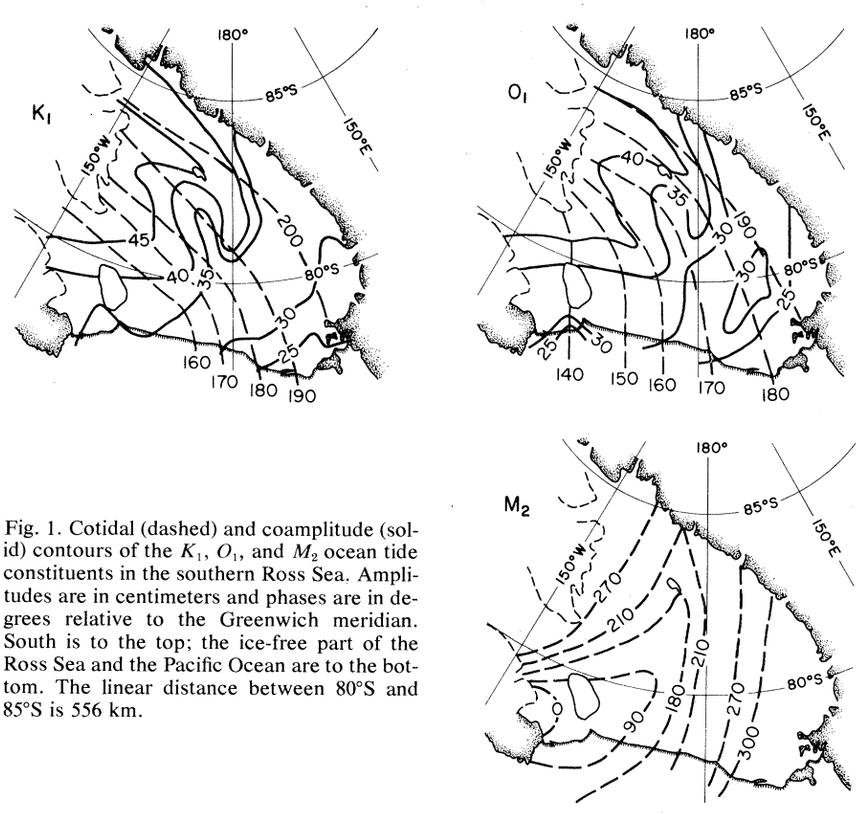

Fig. 1. Cotidal (dashed) and coamplitude (solid) contours of the K_1, O_1, and M_2 ocean tide constituents in the southern Ross Sea. Amplitudes are in centimeters and phases are in degrees relative to the Greenwich meridian. South is to the top; the ice-free part of the Ross Sea and the Pacific Ocean are to the bottom. The linear distance between 80°S and 85°S is 556 km.

0036-8075/79/0202-0443$00.50/0